

Use of K_A -Band for Radio Metric Determinations

P. D. Potter

Radio Frequency and Microwave Subsystems Section

An article in the previous Progress Report (42-57) introduced an FY-80 study being conducted at JPL to assess the applicability of the 32 GHz K_A -band frequency region to planetary exploration, and considered in detail the use of the DSN 64-m antenna network at 32 GHz. The emphasis in that reporting was on increased communications link capacity by use of K_A -band rather than the presently used X-band. In this article, the use of K_A -band to alleviate the radio metric degradation caused by charged particles is discussed.

I. Introduction

The results of a study of the use of the DSN 64-m antenna network at K_A -band have been previously published (Ref. 1); no serious difficulty is envisioned in obtaining good antenna aperture efficiency and the requisite pointing capability. Although interest in K_A -band is primarily motivated by considerations of communications rate improvement and/or spacecraft antenna size reduction, the possibility of grossly reducing the deleterious effects of charged particles on radio metric data is intriguing. It is reasonable to assume that future interplanetary missions will require more precise navigation than is presently being realized, and further that these increased accuracies will be achieved by improvements in virtually all areas, including charged particle effects. While charged particle effects are not presently the dominant navigation error source, the situation might be rather different 10 years from now when the K_A -band link capability may have been implemented.

When the K_A -band frequency region is implemented, it may turn out that the first applications are radio metric rather than related to communications capability. As an example of how a minimal but effective K_A -band radio metric system

could be achieved, a Voyager-sized spacecraft antenna with a raw (unprocessed) power input of 0.5 watt could transmit from the planet Pluto (at its maximum range) to a 64-m antenna on Earth and produce a 10 dB signal-to-noise ratio in a 5 Hz tracking loop. This calculation assumes an overall spacecraft efficiency of 0.13, a ground efficiency of 0.27, a ground antenna elevation angle of 30 degrees, and nominal cloudy atmospheric conditions.

Apart from the interplanetary navigation application, radio metric science is becoming of ever-increasing interest. Studies of the basic properties of space, time, matter and their interrelationships are a major scientific effort. Interplanetary doppler measurements appear to offer an unusual opportunity for detection of the gravity waves predicted by general relativity (Refs. 2-5). Although it is difficult to predict the frequency of detectable gravity waves passing through the solar system (Ref. 5), the first unequivocal detection of such a spacetime disturbance will be a major scientific event. As pointed out by Thorne (Ref. 2), the ability to reliably detect gravity waves would open up a new window onto the universe, a tool for studying those astrophysical phenomena that are poorly reported to Earth by electromagnetic waves.

II. Effect of the Earth Ionosphere

The effect of the Earth ionospheric charged particles on radiowave propagation has been reviewed in detail by Lawrence

et al. (Ref. 6). For radio metric considerations, the quantity of primary interest is the refractive index n (the ratio of vacuum light velocity to phase velocity), which at microwave frequencies is given by (Ref. 6),

$$n = \left[1 - \frac{\left(\frac{\omega_p^2}{\omega^2} \right)}{1 - \frac{1}{2} \frac{\omega_H^2 \sin^2 \theta}{\omega^2 \left(1 - \frac{\omega_p^2}{\omega^2} \right)} \pm \frac{1}{4} \left(\frac{\omega_H^4 \sin^4 \theta}{\omega^4 \left(1 - \frac{\omega_p^2}{\omega^2} \right)^2} + \frac{\omega_H^2 \cos^2 \theta}{\omega^2} \right)^{1/2}} \right]^{1/2} \quad (1)$$

where

- ω = angular frequency of the wave
- $\omega_p = (Ne^2/\epsilon_0 m)^{1/2}$ = angular plasma frequency
- $\omega_H = \mu_0 He/m$ = electron angular gyro frequency
- θ = angle between wave normal and geomagnetic field
- N = free electron number density
- e = electron charge
- m = electron mass
- H = geomagnetic field intensity
- ϵ_0 = free space electric permittivity
- μ_0 = free space magnetic permittivity

The \pm sign in the denominator of Eq. (1) pertains to the ordinary and extraordinary wave indices of the refraction. At X- and K_A-bands the gyro frequency ω_H (of order 10^7 radians/sec) is small compared to ω and Eq. (1) is well approximated by,

$$n \approx \left[1 - \frac{\left(\frac{\omega_p^2}{\omega^2} \right)}{1 \pm \frac{\omega_H \cos \theta}{\omega}} \right]^{1/2} \quad (2)$$

or since $\omega_p \ll \omega$,

$$n \approx 1 - \frac{1}{2} \left(\frac{\omega_p^2}{\omega^2} \right) \left(1 \mp \frac{\omega_H \cos \theta}{\omega} \right) \quad (3)$$

Generally the last term in Eq. (3) can be neglected, resulting in an expression which is isotropic, independent of the geomagnetic field and a function of only the electron density and the frequency of operation. The change in phase path-length, $\Delta \ell$, caused by the ionosphere, is given by,

$$\Delta \ell = \int_0^\infty (n - 1) dl \approx - \frac{b}{\omega^2} \int_0^\infty N dl \quad (4)$$

where

$$b = \frac{e^2}{2\epsilon_0 m} = 1.6 \times 10^3 \text{ (MKS Units)}$$

The radio metric advantage in using a higher frequency is clearly evident in Eq. (4), since uncorrected doppler data will produce the error $\Delta \ell$, and corrected data some fraction of $\Delta \ell$. As the free space light velocity is the geometric mean of phase and group velocities, it is easily shown that a ranging system will produce an opposite error, $-\Delta \ell$. This is the underlying principle of the DRVID (Differenced Range Versus Integrated Doppler) technique for charged particle calibration (Ref. 7).

A complicating feature of the ionospheric effect is that it is rapidly time variant, due both to the changing antenna elevation angle and the varying effect of the sun on the electron density. Thus for missions involving reasonably long light times, the ionospheric effect may be rather different for the transmitted and received signals (posing a problem for the S-X correction technique at least until the advent of an

X-band uplink). Also, the effect is different at different DSN stations, thus complicating the interpretation of certain types of data such as 3-way mode and VLBI.

Roughly speaking, the value of Δl (Eq. 4) at X-band (8.5 GHz) is 1 cm to 1 m, depending on antenna elevation angle and local ionospheric conditions. Because of the inverse-square frequency dependence displayed in Eq. (4), the ionospheric delay, Δl , at K_A -band is typically a millimeter or less and always less than a few centimeters. Together with Faraday rotation, DRVID, and K_A -X-band dual frequency calibration techniques, use of K_A -band would render ionospheric effects virtually negligible.

In summary it can be said that the ionosphere represents a serious radio metric problem for which no good solution presently exists, other than an increase in frequency (such as to K_A -band). Use of tracking stations not on the Earth's surface has been investigated in detail (Ref. 8) and is not economically viable for the foreseeable future.

III. Effect of the Solar Plasma

The solar electron flux affects microwave propagation in the same way as the Earth's ionosphere; thus, the equations in the preceding section are directly applicable. A brief overview of solar plasma effects was recently published by Callahan (Ref. 9). Table 1 (based on Ref. 9) shows typical plasma properties as a function of distance from the center of the sun, in solar radii. For comparison, the Earth ionosphere is also included. Even close to the sun the effect of the solar magnetic field is small (i.e., the gyro frequency is less than 1 MHz) and the last term in Eq. (3) may be neglected. Although the plasma frequency is less than that of the Earth ionosphere, the integrated plasma effect (see Eq. 4) can be larger because of the large range involved.

Not surprisingly, the solar plasma density has a roughly inverse-square dependence on distance from the sun (Ref. 10). Thus for mission times during which the signal passes near the sun, severe doppler noise is encountered even at X-band. Figure 1 is from a JPL internal document and has been modified by adding X- and K_A -band curves, using inverse-frequency scaling¹ as suggested by A. L. Berman of the JPL Telecommunications and Data Acquisition Engineering section. In Fig. 1, the Viking data were obtained during the 1976-1977 solar conjunction and are for a 60-second doppler sample interval. The advantage of using an X- K_A -band frequency

pair for plasma effect calibrations rather than the presently-used S-X-band pair is clearly shown.

The effect of gravity waves on spacecraft doppler data was analyzed by Estabrook and Wahlquist (Ref. 4). The astronomical significance of such gravity wave tests and some of the tracking system performance requirements were discussed by Thorne and Braginsky (Ref. 5), who pointed out the importance of reducing the effect of charged particle dispersion. The philosophical importance of gravity wave detection has been emphasized by Thorne (Ref. 2). The doppler gravitational wave detection experiment has been translated into DSN performance requirements by Berman (Ref. 11). Based on expected gravity wave characteristics (Refs. 4 and 5), Berman selects solar-wind-induced maximum fractional frequency fluctuation values of 3×10^{-16} and 3×10^{-18} for minimal and desired experiments, respectively. According to Berman's calculations (Ref. 12), simultaneous two-way X-band and S-band will be required to support the minimal experiment; even more advanced techniques will be required for the desired experiment. The doppler noise improvement expected to be obtained with an X-band uplink has been discussed by Berman (Ref. 13). Figures 2 and 3 (from Ref. 13) show the expected performance levels for sun-earth-probe angles of 90° and 180° (gravity wave experiment), respectively. While these performance levels are impressive, they do not appear to be satisfactory for the gravity wave experiment.

It is clear from the discussion above that the use of K_A -band for enhancement of radio metric data by reduction of the solar plasma effect would be most desirable, and may be necessary to gravity wave experiments.

IV. Effect of the Troposphere

The Earth troposphere is of great concern to radio metric determinations because its microwave index of refraction differs by about 3×10^{-4} from unity. Moreover, its index of refraction is highly sensitive to water content along the ray-path, which can only be crudely predicted from conditions at the tracking station. Unlike the effect of charged particles, the index of refraction deviation caused by the troposphere is very nearly independent of frequency in the microwave region, as discussed below.

A very general treatment of the tropospheric index of refraction is given by Kerr (Ref. 14). The following relationship between index of refraction and attenuation is valid for virtually any medium, including gases, clouds, and rain:

$$n^2(f) - 1 = \left(\frac{10^{-6}}{\text{LOG}_{10} e} \right) \left(\frac{\lambda}{\pi^2} \right) \int_0^\infty \frac{\alpha(f') f' df'}{(f')^2 - f^2} \quad (5)$$

¹This scaling factor arises from the fact that the plasma path length effect varies inversely with the square of the frequency (Eq. 4) and that the phase per unit length varies directly with frequency. For most applications, path length (inverse-square) is more relevant than phase.

where

f = frequency

$n(f)$ = index of refraction

λ = wavelength in cm

$\alpha(f)$ = attenuation in dB/km

e = natural logarithm base

It can be seen qualitatively from Eq. (5) that very large values of attenuation would be necessary to result in a significant variation in n . At 32 GHz, for example, an α value of 1.6 dB/km would be necessary to cause a variation of 10^{-3} in $n^2 - 1$ (Ref. 14, p. 645).

A careful measurement of the dielectric constant water vapor² at 9.3 and 24.8 (near the absorption resonance) GHz was reported by Birnbaum and Chatterjee (Ref. 15). With a probable error of approximately 1 percent in their measurements, they could detect no difference between the dielectric constants at these two frequencies, for a variety of temperatures and pressures. Similarly, Smith and Weintraub (Ref. 16) stated that the index of refraction of the atmosphere is independent of frequency to 30 GHz to within 0.5 percent.

Recently Berman and Slobin (Ref. 17) have discussed the expected tropospheric path length fluctuation at DSN sites and its application to gravity wave detection. They derive a typical two-way fractional frequency fluctuation value (1000 second averaging time) of 1.6×10^{-14} . Since this is larger compared to the required values (see Section III above), calibration techniques such as the water vapor radiometer are proposed.

In summary it can be said that the troposphere represents a severe problem for radio metric measurements, but appears to be amenable to calibration techniques which have not yet been implemented. In this section it has been shown that the effect is essentially frequency-independent and that thus these techniques will be as equally efficacious at K_A -band as they are at S- and X-bands.

²Index of refraction is proportional to the square root of the dielectric constant.

V. Hardware Considerations

In general, the electronic system can be designed such that hardware imperfections do not degrade the radio metric performance. For example, the spectral purity (frequency stability) of the ground transmitter should be a significant function of the frequency and timing base (the hydrogen maser) only, and phase lock loop tracking noise can be controlled by bandwidth/SNR control.

Thus, while electronic stability will be a more serious design constraint at K_A -band than it is at X-band (for example in the ground power amplifier and the spacecraft multiplier stages), this problem is amenable to a state-of-the-art engineering solution.

Two microwave hardware problems are worth considering. The first is microwave delay variation caused by imperfections in the large ground antenna. This problem has been studied in detail by Cha, et al. (Ref. 18). They found that, for example, small (~ 1 cm) movements of the antenna sub-reflector could cause delay variations of several tenths of a nanosecond. This result is, however, largely frequency independent and should not affect a decision to use K_A -band for radio metric purposes.

Secondly, the low noise maser amplifier in the ground receiving system is of concern since it has a large group delay. The stability of this delay has been determined for typical S- and X-band DSN equipment (Ref. 19, 20 and 21); typical stability over the time of one pass is $\pm 3^\circ$ phase and ± 0.3 nanosecond group delay. No significant differences exist between S- and X-band data, implying a design of frequency independence and similar performance for a K_A -band maser system.

VI. Conclusion

Those aspects of radio metrics which are relevant to the possible future use of K_A -band deep space-to-earth and earth-to-deep-space links have been reviewed. From the standpoint of reducing the harmful effects of charged particles, the use of K_A -band appears highly desirable.

Acknowledgment

Many valuable comments on the solar plasma effect were made by A. L. Berman of the JPL Telecommunications and Data Acquisition Engineering Section.

References

1. P. D. Potter, "64-m Antenna Operation at K_A -Band," *The Telecommunications and Data Acquisition Progress Report 42-57*, June 15, 1980.
2. K. S. Thorne, "Gravitational Wave Detection with the Solar Probe: I. Motivation," in *A Close-Up of the Sun*, JPL Publication 78-70, September 1, 1978, pp. 433-440.
3. F. B. Estabrook, "Gravitational Wave Detection with the Solar Probe: II. The Doppler Tracking Method," in *A Close-Up of the Sun*, JPL Publication 78-70, September 1, 1978, pp. 441-449.
4. F. B. Estabrook and H. D. Wahlquist, "Response of Doppler Spacecraft Tracking to Gravitational Radiation," *General Relativity and Gravitation*, Vol. 6, No. 5, October, 1975, pp. 439-447.
5. K. S. Thorne and V. B. Braginsky, "Gravitational-Wave Bursts from the Nuclei of Distant Galaxies and Quasars: Proposal for Detection Using Doppler Tracking of Interplanetary Spacecraft," *The Astrophysical Journal*, Vol. 204, February 15, 1976, pp. L1-L6.
6. R. S. Lawrence, C. G. Little and H. J. A. Chivers, "A Survey of Ionospheric Effects upon Earth-Space Radio Propagation," *Proceedings of the IEEE*, January, 1964, pp. 4-27.
7. P. F. MacDoran and W. L. Martin, "DRVID Charged-Particle Measurement with a Binary-Coded Sequential Acquisition Ranging System," *JPL Space Programs Summary 37-62*, Vol. II, March 31, 1970, pp. 34-41.
8. J. A. Hunter, *Orbiting Deep Space Relay Station Study Final Report (3 Volumes)*, JPL Publication 79-30, June 15, 1979.
9. P. S. Callahan, "Transmission Media Effects on Precise Doppler Tracking," in *A Close-Up of the Sun*, JPL Publication 78-70, September 1, 1978, pp. 450-456.
10. A. L. Berman, "A Unified Observational Theory for Solar Wind Columnar Turbulence," *The Deep Space Network Progress Report 42-50*, April 15, 1979, pp. 124-131.
11. A. L. Berman, "The Gravitational Wave Detection Experiment: Description and Anticipated Requirements," *The Deep Space Network Progress Report 42-46*, August 15, 1978, pp. 100-108.
12. A. L. Berman, "Solar Wind Density Fluctuation and the Experiment to Detect Gravitational Waves in Ultraprecise Doppler Data," *The Deep Space Network Progress Report 42-44*, April 15, 1978, pp. 189-196.

13. A. L. Berman, "Simultaneous Dual-Frequency, Round-Trip Calibration of Doppler Data with Application to Radio Science Experiments" *The Deep Space Network Progress Report 42-48*, December 15, 1978, pp. 48-54.
14. D. E. Kerr, Ed., *Propagation of Short Radio Waves*, McGraw-Hill Book Company, Inc., 1951, pp. 641-646.
15. G. Birnbaum and S. K. Chatterjee, "The Dielectric Constant of Water Vapor in the Microwave Region," *Journal of Applied Physics*, Volume 23, No. 2, February, 1952, pp. 220-223.
16. E. K. Smith, Jr. and S. Weintraub, "The Constants in the Equation for Atmospheric Refractive Index at Radio Frequencies," *Proceedings of the I.R.E.*, Vol. 41, August, 1953, pp. 1035.
17. A. L. Berman and S. D. Slobin, "Tropospheric Path Length Fluctuation in Temperature Semiarid Locales: Application to the Gravitational Wave Detection Experiment," *The Deep Space Network Progress Report 42-55*, February 15, 1980, pp. 79-85.
18. A. G. Cha, W. V. T. Rusch and T. Y. Otoshi, "Microwave Delay Characteristics of Cassegrainian Antennas," *IEEE Trans. on Ant. and Prop.*, Vol. AP-26, No. 6, November, 1977, pp. 860-865.
19. R. Clauss, E. Weibe and R. Quinn, "Low-Noise Receivers: Microwave Maser Development," JPL Technical Report 32-1526, Vol. XI, Oct. 15, 1972, pp. 71-80.
20. D. L. Trowbridge, "X-Band Traveling Wave Maser Amplifier," *The Deep Space Network Progress Report 42-28*, Aug. 15, 1975, pp. 69-77.
21. J. M. Urech, et al., "S-Band Maser Phase Delay Stability Tests," *The Deep Space Network Progress Report 42-48*, December 15, 1978, pp. 102-117.

Table 1. Plasma properties

| R (R_{\odot}) | Electron density (cm^{-3}) | f_p (Hz) | f_g (Hz) | $(f_p/f_s)^2$ | $(f_p/f_s)^2 R$ (m) | f_g/f_s |
|--|---|-------------------|-------------------|-----------------------|------------------------|----------------------|
| 5 | 2.8×10^4 | 1.5×10^6 | 1.3×10^5 | 2.9×10^{-8} | 9.8×10^1 | 1.5×10^{-5} |
| 10 | 5.3×10^3 | 6.6×10^5 | 3.3×10^4 | 5.4×10^{-9} | 3.8×10^1 | 3.9×10^{-6} |
| 21.6 | 1.1×10^3 | 2.9×10^5 | 7.0×10^3 | 1.1×10^{-9} | 1.6×10^1 | 8.2×10^{-7} |
| 216 | 9.4 | 2.7×10^4 | 7.1×10^1 | 9.8×10^{-12} | 1.4 | 8.6×10^{-9} |
| Ionosphere ($R = 200 \text{ km}$) | 2.0×10^5 | 4.0×10^6 | 8.4×10^5 | 2.0×10^{-7} | 4.3 | 9.9×10^{-5} |

f_p = plasma frequency = $8.98 \times 10^3 N^{1/2} \text{ Hz}$
 f_g = gyro frequency = $2.80 \times 10^6 B \text{ Hz}$

$$n^2 = \frac{1 - f_p^2/f^2 \pm f_g/f}{1 \pm f_g/f}$$
 f_s = signal frequency = 8.5 GHz

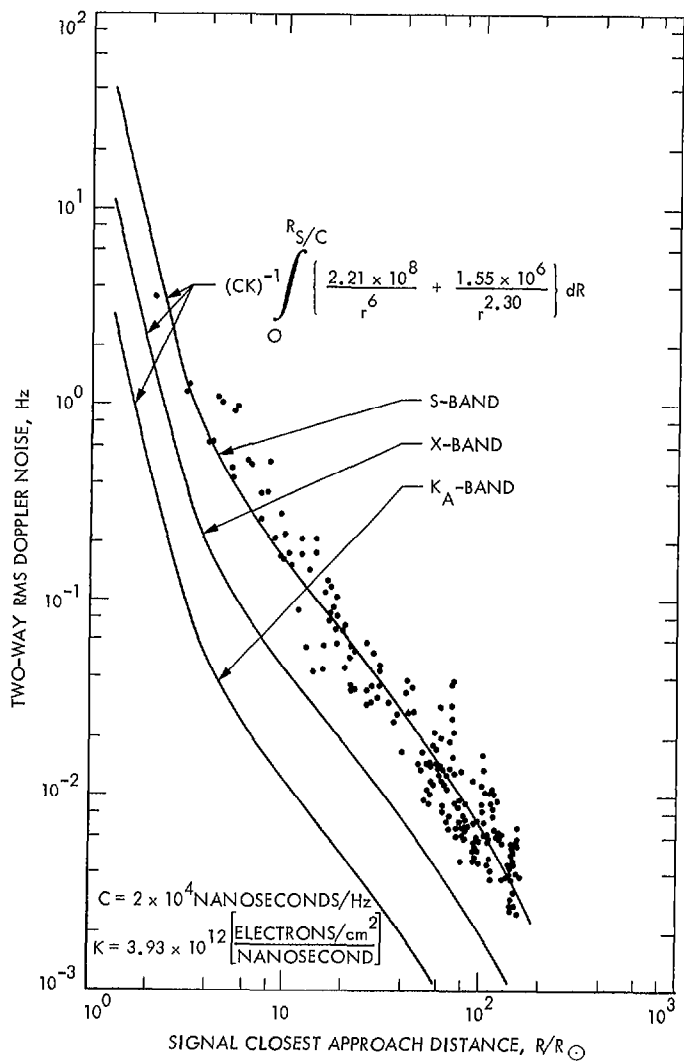


Fig. 1. Doppler phase fluctuation vs signal closest approach to the Sun

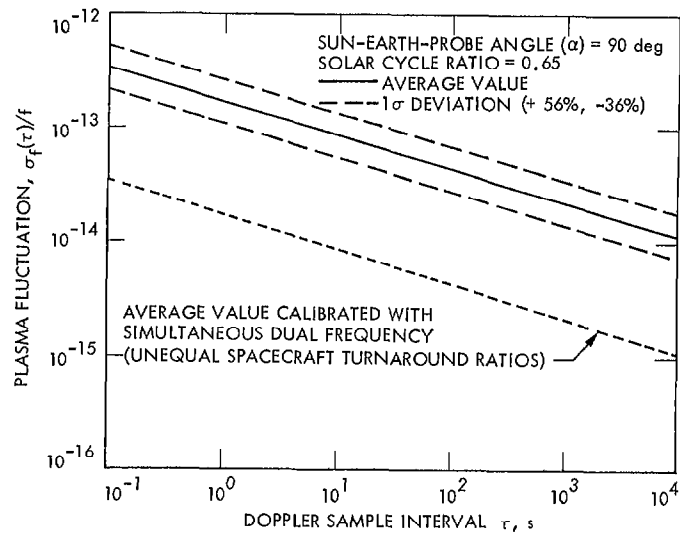


Fig. 2. Two-way X-band plasma fluctuation at solar cycle minimum

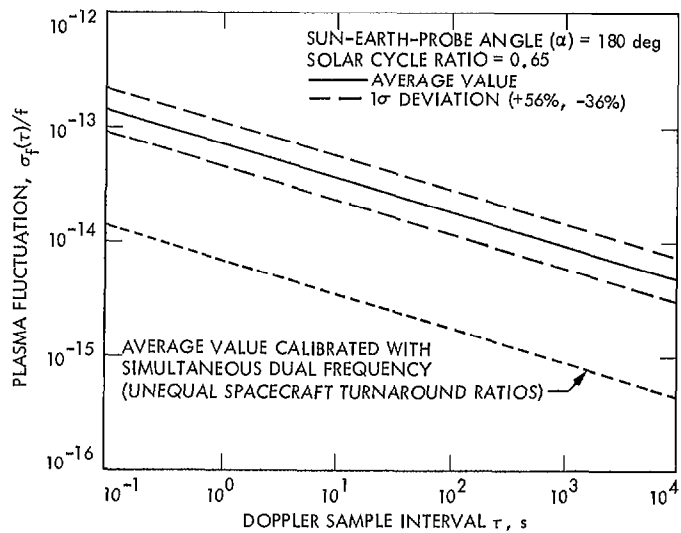


Fig. 3. Two-way X-band plasma fluctuation at solar cycle maximum